POLYMER FLOODING IN SANDPACKS WITH A DUAL-POROSITY

I. Ringen[1,2,3], H. Stiegler[1], O. Nødland[1,2,3], A. Hiorth[1,2,3] and A. Stavland[2,3]

[(1)] University of Stavanger, Norway, [(2)]The National IOR Center of Norway, [(3)]IRIS AS – International Research Institute of Stavanger, Norway

This paper was prepared for presentation at the International Symposium of the Society of Core Analysts held in Snowmass, Colorado, USA, 21-26 August 2016

ABSTRACT

Polymer and low salinity water flooding are methods to improve oil recovery from both sandstone and carbonate reservoirs. Combining these two methods is of interest for at least two reasons. Firstly, this improves both the macroscopic and microscopic sweep efficiency at the same time, and secondly less polymer is needed when it is mixed with a low salinity brine. The last point is important since it reduces the amount of produced chemicals, which has both financial and environmental benefits. However, polymer molecules are large compared to the ions in the brine, and even large compared to the typical pore sizes. The polymer molecules may therefore flow at a completely different speed than the ions. This could be of particular importance in fractured carbonate systems.

In this paper we investigate the rheological behavior of a polymer solution in a system where the full pore system is accessible for ionic transport, while not for the polymer molecules. We have designed a novel experimental setup that allows for electric resistance measurements along the porous media. From the resistivity measurements, information about the porosity and ionic concentrations within the sandpack was gained. A low salinity polymer solution was injected into a dual porosity sandpack saturated with a higher salinity brine. The viscosity of the effluent fluid was monitored with a capillary tube rheometer, and the apparent viscosity in the porous medium was derived from the differential pressure across the column. The flooding experiments showed viscoelastic behavior, i.e. by increasing shear rates, the apparent viscosity increased dramatically due to elongation of the polymers molecules. Most importantly, the experimental results clearly show that the polymer front moves at a higher speed than the salinity front. As a result, the polymer solution mixes with the high salinity brine and the viscosity decreases. These effects are important to take into account when designing polymer floods in dual-porosity systems.

INTRODUCTION

In order to increase the oil recovery, waterflooding has been a successful recovery technique for many oil reservoirs during the last decades. However, in some reservoirs,

waterflooding may lead to early water breakthrough and low oil production rates. Polymer flooding is considered as a very promising technology in enhanced oil recovery (EOR) processes. If polymers are added to the injection water they increase the water viscosity. This can lead to a favorable mobility ratio between oil and water. Depending on the heterogeneities in the reservoir, the change in mobility ratio could greatly impact the macroscopic sweep efficiency and enhance oil recovery. However, polymer solutions are non-Newtonian fluids and hence, the rheological properties are sensitive to shear forces.

In field operations, hydrolyzed polyacrylamides (HPAM) are the most common EOR polymers [1]. These synthetic polymers show viscoelastic properties when flowing through a porous media [1-9]. At low fluid velocities, a Newtonian or near-Newtonian behavior is reported by Seright et.al. [9], while Heemskerk et al. [8] and Delshad et al. [10] reports shear thinning behavior. Both Chauveteau et al. [11] and Stavland et al. [1] demonstrate that the polymer solutions tested exhibit shear thinning behavior with lower viscosities than bulk viscosity because the polymer does not flow through the entire pore volume. At increasing shear rates, the polymer molecules get elongated and contracted due to the pore structures of the porous media. Consequently, the apparent viscosity of the polymer solution increases dramatically (usually named a shear thickening behavior). If the polymer solution is exposed to very high stresses, the molecules may rupture and degrade [1]. This could easily happen when the polymer is injected, if care is not taken.

The properties of polymer solutions are affected by the molecular weight, polymer concentration and salinity. Polymers are polyelectrolytes, i.e. the molecules have multiple charges distributed along the chain, hence, in low salinity brines the molecules expand due to mutual repulsion of charges along the molecule chain [12]. This repulsion increases the viscosity of the solution, and consequently less chemicals are needed to obtain the targeted viscosity. In recent years, it has been observed that the salinity of the injected fluid in itself can increase the microscopic sweep efficiency of oil reservoirs [13]. By mixing polymers in low salinity brines, it is possible to obtain an increase in both macroscopic and microscopic sweep efficiency. However, the polymer molecules and ions move with different speeds in the porous media, mainly because the polymer molecules are larger than the ions. This could have the effect that the polymer molecules leave the low salinity brine behind and consequently mixes with the formation water, and part of the benefit with injecting polymers in low salinity water is lost.

To shed some more light on this phenomenon, we have flooded polymer solutions with different salinities through a sandpack column. This column consisted of silica grain, where the grains themselves are porous. This system has to our knowledge not been used to study the flow of polymer flow before. Every individual grain consists of consolidated micro silica, thus there is a macro porosity between the grains and a micro porosity within the grains. As a consequence of the macro and micro porosity the full pore volume was accessible for ionic transport but not for the polymer molecules. Electric resistance was measured along the column to track ionic concentrations during the flooding

experiments. The effective polymer rheology was measured in the sandpack, and a capillary tube rheometer, at the outlet of the sandpack, monitored the effluent polymer rheology.

THEORY

In bulk, the polymers have a shear thinning behavior. The viscosity, η, decreases with increasing shear rate, $\dot{\gamma}$, and the behavior is well described by a Carreau model [14],

$$\eta(\dot{\gamma}) = \eta_\infty + (\eta_0 - \eta_\infty) \cdot [1 + (\lambda_1 \dot{\gamma})^x]^{(n-1)/x}, \quad (1)$$

where η_0 and η_∞ is the polymer viscosity at zero and infinite shear rate, respectively, λ_1 is a time constant representing the critical shear rate at which the fluid deviates from Newtonian behavior, and n is the flow behavior index. For a shear thinning fluid, $n < 1$ and n typically ranges from 0.4 to 0.7 [15]. The tuning parameter, x, is used to improve the viscosity match.

Viscous flow in capillary tubes

A capillary tube was used to measure the effluent viscosity. In order to allow for a simple interpretation of the measured pressure drop across the capillary tube and the imposed flow rate, it is important to choose a tube with a diameter much larger than the polymer molecules to ignore wall effects, and a long tube to avoid entrance and exit effects. If an appropriate tube is chosen, the flow is well described by the Hagen-Poiseuille equation. In such a flow, the shear stress, τ, is given as

$$\tau = \frac{\Delta P r'}{2L}, \quad (2)$$

where ΔP is the differential pressure, r' is the radius, and L is the tube length. For a Newtonian fluid, the shear stress is related to the shear rate through $\tau = \eta\dot{\gamma}$. Here, the shear rate, $\dot{\gamma}$, is defined as

$$\dot{\gamma} = \frac{dv(r')}{dr'}, \quad (3)$$

where v is the flow velocity along the tube. Assuming a power-law shear rate, i.e. ignoring η_∞ and assuming $\lambda_1\dot{\gamma} \gg 1$, the viscosity of the polymer solution in the capillary tube follows a simple power law, $\eta = \eta_0(\lambda_1\dot{\gamma})^{n-1}$. Combining the two equations above, solving for $v(r')$, and then integrating over the cross section of the tube with radius R, we get the flow rate, q. We can then express the apparent shear rate, $\dot{\gamma}_A$, in the tube and apparent viscosity, η_A, as

$$\dot{\gamma}_A = \frac{3 + 1/n}{4} \cdot \frac{4q}{\pi R^3} \quad \text{and} \quad \eta_\mathrm{A} = \frac{4}{3 + 1/n} \cdot \frac{\pi R^4 \Delta P}{8qL}, \quad (4)$$

respectively. The $(3 + 1/n)/4$ term is known as the Mooney-Rabinoswitch-Weissenberg correction factor that takes into account the effect of the change of shape of the velocity profile when non-Newtonian fluids flow through capillaries under laminar conditions. For Newtonian fluids ($n = 1$), equation (4) reverts to the usual Hagen-Poiseuille equation.

Apparent viscosity in porous media

The viscosity of the polymer solution cannot be measured directly in flooding experiments. Due to the complex network of pores and channels in the porous medium, the shear rate and thus the viscosity will vary within the medium. In this work we will extend the formulation developed in the previous section by introducing an average radius defined by the Kozeny-Carman relationship $k = \phi \frac{r^2}{8\tau_c}$ (τ_c is the tortuosity):

$$\dot{\gamma} = \alpha \cdot \frac{4q}{A\sqrt{8k\phi}}. \tag{5}$$

Here A is the cross-sectional area, k is the permeability, ϕ is the porosity of the porous medium, and α is an empirical parameter used to match viscosity measured in bulk and porous medium, normally set equal to 2.5 [1]. The arguments for $\alpha > 1$ are that the permeability to the polymer is lower than to water and that the polymer velocity is higher than to water. The advantages of using this model is its simplicity and clarity, but clearly it has its limitations due to the dual-porosity of the system. We have therefore used the macro porosity ($\phi = \phi_{\mathrm{mac}}$), since the polymer molecules are too large to flow in the narrow micro pores.

The apparent viscosity is estimated from the Darcy equation,

$$\eta_{\mathrm{A}} = \frac{Ak}{q}\frac{\Delta P}{\Delta L}. \tag{6}$$

Since the effective shear rate is proportional to the flow velocity, several models have been suggested for the viscosity as a function of flow rate and properties of the porous medium. Based on the Carreau model, Stavland et.al. derived a model for the apparent viscosity of polymers in porous media where the apparent viscosity is the sum of the shear viscosity and elongation viscosity multiplied by a degradation term [1]:

$$\eta_{\mathrm{app}} = \eta_\infty + \left[(\eta_0 - \eta_\infty) \cdot (1 + (\lambda_1\dot{\gamma})^n) + (\lambda_2\dot{\gamma})^\xi\right] \cdot [1 + (\lambda_3\dot{\gamma})^x]^{\frac{\xi - 1/2}{x}}. \tag{7}$$

The first part of equation (7) represent the bulk viscosity matched with the Carreau model (1). The next term, $(\lambda_2\dot{\gamma})^\xi$, represents the elongation viscosity, which increases dramatically by increasing the shear rate. The elongation exponent, $\xi > 0$, depends on molecular weight of the polymer. As we see from the expression, this elongation term is increasing for shear rates higher than $1/\lambda_2$, and the onset of elongation depends on the porous medium,

$$\frac{1}{\lambda_2} = N_{\mathrm{De}}\left(\frac{1-\phi}{\phi}\right)\frac{6\alpha\sqrt{\tau_c}}{\lambda_1}, \tag{8}$$

where N_{De} is the Deborah number describing the liquid-like behavior of the polymer. The last term in equation (7) represents the degradation of polymers, where the time constant λ_3 represents the onset of shear degradation and x is a tuning parameter used to improve viscosity match.

Chemical concentrations and resistivity

In this work we use resistance measurements to track concentration fronts in the sandpack. The resistivity, ρ, is the inverse of the conductivity, σ, and the relationship between resistivity and resistance is

$$r = \rho \frac{L}{A}, \tag{9}$$

where r is the resistance, L is the length and A is cross-sectional area of the porous media. The total resistance of a fluid-filled porous media, r_{T}, can be represented by the parallel resistance relationship, and since most rocks are non-conductive, the total resistance of a fluid-filled porous medium is related to the brine resistance ($r_{\mathrm{T}} \approx r_{\mathrm{w}}$). A fluid's ability to conduct electric current depends strongly on its ionic concentration. The most common approach to link resistance to concentration is to use Archie's law [16],

$$\sigma_{\mathrm{o}} = \frac{1}{F}\sigma_{\mathrm{w}}. \tag{10}$$

Here, σ_{w} is the conductivity of the brine, σ_{o} is the conductivity to the fluid-filled porous medium, and F is the formation factor, $F = \phi^{-m}$, which is related to the total porosity via the cementation exponent m. The total porosity, ϕ_{T}, of the sandpack is

$$\phi_{\mathrm{T}} = \phi_{\mathrm{mac}} + \phi_{\mathrm{mic}}\,, \tag{11}$$

where ϕ_{mac} is the macro porosity and ϕ_{mic} is the micro porosity. Here we use the following generalization of Archie's law for a dual porosity medium [17]:

$$\sigma_{\mathrm{o}} = \phi^{m-1}\left(\phi_{\mathrm{mac}}\sigma_{\mathrm{w,mac}} + \phi_{\mathrm{mic}}\sigma_{\mathrm{w,mic}}\right). \tag{12}$$

In the case where the conductivity of the two domains are equal, $\sigma_{\mathrm{w,mac}} = \sigma_{\mathrm{w,mic}} = \sigma_{\mathrm{w}}$, equation (12) reduces to (10). From our experiments, conductivity versus salinity is,

$$\sigma_{\mathrm{w}} = a\, c_{\mathrm{NaCl}} + b, \tag{13}$$

where c_{NaCl} is the salinity of the brine in [g/cm^3]. From our experiments, $a = 1463$ mS.cm^2/g and $b = 2.03$ mS/cm.

MATERIALS AND METHODS

In the experiments, two brines were used, 35 g/L NaCl (B35) and 10 g/L NaCl (B10), where the latter was the polymer make up brine. The brines were filtered using a 0.45 μm HAWP-filter from Millipore. The polymer was Flopaam 5115SH, a synthetic acrylate-ATBS polymer with medium anionicity and high molecular weight, delivered by SNF. A 5000 ppm mother solution was prepared by gently adding the polymer in the brine under high rate mechanical mixing, thereafter overnight low rate mixing. Dilution to 1000 ppm was performed using a magnetic stirrer. Bulk viscosity was measured using an Anton Paar Physica MCR 301 rheometer at 20 °C and variable shear rates from 0.1 s^{-1} to 500 s^{-1} using a cone and plate geometry. Viscosities were measured at both increasing and decreasing shear rates. Due to better accuracy in the measurements, the viscosities

obtained at decreasing shear rates were used. In Table 1 and Table 2, the fluid properties and the conductivity of the NaCl brines is shown.

For the sandpack column, Silica Gel 63-200 μm was used as sand. In Figure 1, Scanning Electron Microscope (SEM) images of the grain structure are shown. The micro structure is clearly visible; each individual sand grain is porous as the grains are consolidations of multiple micro silica grains. The size of a micro grain is approximately 80 nm with a pore size of 6 nm. The density of Silica is 2.65 g/cm^3. From the supplier, Sigma-Aldrich, the pore volume of the macro grains was reported to be 0.8 cm^3/g rock, thus the micro porosity was estimated to 38 % (36.3-41.3 %) and the macro porosity to 44 % (39.2-46.6 %), based on 12 sandpacks. The properties of the column sandpack are shown in Table 3.

The column used was an 80 cm long construction of 6 glass cylinders and metal joints as illustrated in Figure 2. The dimensions of the glass cylinder were D = 1.6 cm and L = 10 cm. This construction allows for measurements of electric current along the sandpack during flooding. An automatic RCL meter was connected to the column by 7 electrodes on the metal joints, which measured the 6 sections (Z1–Z6).

Experimental procedure

A schematic drawing of the experimental set-up is shown in Figure 2. Several sandpack columns were flooded with P10 during this work. All experiments were performed at ambient temperature. To control the pressure in the system, a backpressure regulator, set to 3 bars, was set up at the end of the system. To measure the viscosity of the effluent during flooding, a capillary tubing acting as a rheometer was connected to the outlet of the column. The capillary tube rheometer was 100 cm long with an inner diameter of 0.0762 cm. The flooding process was as follows:

1. Assemble the column. Successful packing was achieved by filling sand from the top of the column while the outlet was connected to a vacuum pump. Vibration during packing was not an option due to the glass construction.
2. Saturate the sandpack with brine B35 at the injection rate 1 ml/min.
3. Measure the porosity from the sandpack saturation (pore volume injected), and from mass measurements of the sand grains.
4. The effective brine permeability was determined by varying the injection rates and using the corresponding differential pressures across the column in equation (6).
5. In one separate sandpack/experiment, B10 was injected for evaluating ion dispersion in a brine-brine displacement experiment. The effluent ionic concentration was estimated by measuring Cl^- content.
6. In the following experiment, the polymer solution P10 was injected at a constant rate of 0.3 ml/min. This injection rate corresponds to the shear rate of ~60 s^{-1} in the sandpack and ~115 s^{-1} in the capillary tube rheometer.
7. Measure the pressure drop across the sandpack at different injection rates for estimating the apparent viscosity of the polymer solution within the sandpack.

8. Measure fluid effluent viscosity by measuring the pressure drop across the capillary tube rheometer connected to the outlet of the column. The injection rate was altered and effluent viscosity was recorded at stable differential pressure.
9. During all flooding experiments, the electrical resistance over 6 section (Z1–Z6) was continuously measured to track chemical concentration profiles.

RESULTS AND DISCUSSION

As the sandpacks comprises of porous silica grains, the total porosity is high, approximately 80 %. The total porosity, ϕ_{T}, includes the macro porosity, ϕ_{mac} , and the micro porosity, ϕ_{mic} , see equation (11). We clearly see the effect of the micro and macro porosity in Figure 3. In Figure 3, the effluent concentration is shown from one experiment where B35 was displaced by B10 at the injection rate of 2 ml/min. Effluent samples were collected to determine the ion concentration, where the Cl^- concentration was determined by titration with $AgNO_3$. Injection of at least 2.5 pore volumes of B10 was required to displace all initial ions, which we interpret as being caused by the dual-porosity structure. A possible explanation could be that the time it takes to flow through the macro pores is shorter than the time it takes to exchange ions from the micro pores. Consequently, a long concentration tail is observed. The electrical resistance measurements along the sandpack also support this, as can be seen in Figure 4. In this figure, the measured resistance has been calculated to NaCl concentration by the relation in equation (13). When the initial high salinity brine B35 is displaced by either the low salinity brine B10 or the polymer solution P10, the electrical resistance increases for every section as the front propagates though the sandpack. In Figure 5, the measured resistances for the 6 sections are plotted versus pore volume injected of P10, along with simulated values. As the front propagates there is an increasing lag before the resistivity reaches the expected plateau value.

In our view, the most interesting results is when the polymer solution was injected in the system. In Figure 6, the bulk properties of the polymer solutions are shown. There is a clear effect of the salinity of the make up brine. As seen, the measured viscosity for P10 and P35 are well matched with a Carreau model, where the shear thinning exponent n is 0.72 and 0.83 for P10 and P35, respectively. In Figure 7, the results from the capillary tube rheometer in 3 different sandpacks is shown and we see that there is a good match between the bulk measurements and the capillary tube rheometer. The viscosity of the low salinity P10 solution was higher than the viscosity of P35. At low salinities, the polymer molecules can expand due to electrostatic repulsion between the anionic groups along the polymer chain [15]. This results in a higher viscosity for the low salinity polymer solution. When the salinity is increased, the repulsive forces are reduced. This decreases the polymer chain and hence, the viscosity is decreased.

In Figure 8, the pressure drop across the capillary tube rheometer and the corresponding resistance measurements are shown when the low salinity polymer solution, P10, displaced the high salinity brine, B35. At PV = 0.58, the polymer breaks through, as seen by the increased differential pressure across the capillary tube rheometer. The apparent

viscosity of effluent between 0.58 and 1.0 pore volume injected is ~4.5 cp at the shear rate 115 s^{-1}. This apparent viscosity is close to the P35 bulk viscosity of 5.5 cp at 115 s^{-1}. The resistance measurements along the sandpack show that the salinity front lags behind, and from the resistance measurements in the last section (Z6) of the column, the salinity is high when the polymer leaves the sandpack. At approximately 1 PV injected, the low salinity water breaks through. When this happens, we see an increase in the resistance, and more importantly a second increased pressure drop occurs across the capillary tube. The apparent viscosity of the effluent after 1 PV injected is ~6.2 cp, which is close to the bulk viscosity of 7.0 cp at 115 s^{-1} for P10. This clearly demonstrates the different flow paths taken by the ions and the polymers through the column. The fraction of the macro pore volume to the total pore volume is 0.58, and because of this, $u_{\mathrm{polymer}}/u_{\mathrm{NaCl}} \approx 1.72$. A second run in the same column was performed to determine if there was any effect of polymer retention, see Figure 9. In Figure 9, the pressure drop across the sandpack is shown together with the pressure drop across the capillary tube rheometer at the outlet of the column. Within the experimental limits we could not observe any retention.

In Figure 10, the apparent viscosity in the column given by equation (6), is shown together with the estimated viscosity from the capillary tube rheometer when the polymer solution P10 was injected through the sandpack at various flow rates. All the experiments/sandpacks show the same trends: By increasing the shear rates, shear thickening behavior was observed and the apparent viscosity increased from a shear rate of 100 s^{-1}. This behavior is caused by elongation of the polymer molecules in the pore structure of the sandpacks. This elongation effect is well-known and well documented in the literature [1, 8, 9]. A further increase in shear rates could have ruptured the molecules, but shear degradation was not observed due to pressure limitations in the system. The results were well matched with the Carreau-based apparent viscosity model given in equation (7), by adjusting the shear elongation term. We were also able to match the experiments at $S_w = 1 - S_{or}$, see Figure 11.

CONCLUSION

The rheology behavior of the synthetic acrylate-ATBS polymer solution is affected by ionic concentration and shear. In bulk measurements, the polymer solution shows shear thinning behavior, while in the sandpack both shear thinning and shear thickening was observed. As the shear rates increases, the apparent viscosity increases dramatically due to elongation of the polymer molecule. The apparent viscosity is dependent on the effective porosity and permeability of the porous medium.

In a dual porosity system, the polymer molecules flow with higher velocity than the salinity front, i.e. the polymers flow in the macro pores, while the ions are transported (mainly by diffusion) in the entire pore volume. The polymer front mixes with the initial brine, hence the viscosity of the front decreases. When the initial ions are fully displaced, the viscosity of the polymer solution increases.

The difference in flow velocity is important to consider when evaluating the EOR potential of polymer flooding on field scale, e.g. in highly inhomogeneous reservoirs. The reservoir formation water is typically more saline than the injected water, which usually is seawater (on the Norwegian Continental Shelf). Thus, if the flow velocity of polymers is higher than the velocity of the salinity front, the polymer will mix with formation water and consequently the viscosity will be decreased. This does not mean that there is not a potential benefit by combining polymer and low salinity flooding. We have not at all considered the effect of low salinity water on the microscopic sweep efficiency which can be substantial.

ACKNOWLEDGEMENTS

The authors acknowledge the Research Council of Norway and the industry partners; ConocoPhillips Skandinavia AS, BP Norge AS, Det Norske Oljeselskap AS, Eni Norge AS, Maersk Oil Norway AS, DONG Energy A/S, Denmark, Statoil Petroleum AS, ENGIE E&P NORGE AS, Lundin Norway AS, Halliburton AS, Schlumberger Norge AS, Wintershall Norge AS of The National IOR Centre of Norway for support.

REFERENCES

1. Stavland, A., H. Jonsbraten, A. Lohne, A. Moen, and N.H. Giske. Polymer Flooding - Flow Properties in Porous Media versus Rheological Parameters. *Society of Petroleum Engineers.* 2010. DOI: 10.2118/131103-ms.
2. Pye, D.J., *Improved Secondary Recovery by Control of Water Mobility.* 1964.
3. Smith, F.W., *The Behavior of Partially Hydrolyzed Polyacrylamide Solutions in Porous Media.* 1970.
4. Jennings, R.R., J.H. Rogers, and T.J. West, *Factors Influencing Mobility Control By Polymer Solutions.* 1971.
5. Hirasaki, G.J. and G.A. Pope, *Analysis of Factors Influencing Mobility and Adsorption in the Flow of Polymer Solution Through Porous Media.* 1974.
6. Seright, R.S., *The Effects of Mechanical Degradation and Viscoelastic Behavior on Injectivity of Polyacrylamide Solutions.* 1983.
7. Masuda, Y., K.-C. Tang, M. Miyazawa, and S. Tanaka, *1D Simulation of Polymer Flooding Including the Viscoelastic Effect of Polymer Solution.* 1992.
8. Heemskerk, J., R. Rosmalen, R. Janssen-van, R.J. Holtslag, and D. Teeuw. Quantification of Viscoelastic Effects of Polyacrylamide Solutions. *Society of Petroleum Engineers.* 1984. DOI: 10.2118/12652-ms.
9. Seright, R.S., J.M. Seheult, and T. Talashek, *Injectivity Characteristics of EOR Polymers.* 2009.
10. Delshad, M., D.H. Kim, O.A. Magbagbeola, C. Huh, G.A. Pope, and F. Tarahhom. Mechanistic Interpretation and Utilization of Viscoelastic Behavior of Polymer Solutions for Improved Polymer-Flood Efficiency. *Society of Petroleum Engineers.* 2008. DOI: 10.2118/113620-ms.
11. Chauveteau, G., M. Tirrell, and A. Omari, *Concentration dependence of the effective viscosity of polymer solutions in small pores with repulsive or attractive walls.* Journal of Colloid and Interface Science, 1984. **100**(1): p. 41-54.

12. Sorbie, K.S., *Polymer - improved oil recovery* 1991: Springer Science & Business Media.
13. Tang, G.-Q. and N.R. Morrow, *Influence of brine composition and fines migration on crude oil/brine/rock interactions and oil recovery.* Journal of Petroleum Science and Engineering, 1999. **24**(2–4): p. 99-111.
14. Green, D.W. and G.P. Willhite, *Enhanced oil recovery*. SPE textbook series. Vol. vol. 6. 1998, Richardson, Tex: Henry L. Doherty Memorial Fund of AIME, Society of Petroleum Engineers.
15. Sheng, J., *Modern chemical enhanced oil recovery: theory and practice*2010: Gulf Professional Publishing.
16. Archie, G.E., *The Electrical Resistivity Log as an Aid in Determining Some Reservoir Characteristics.* 1942.
17. Singha, K., F.D. Day‐Lewis, and J. Lane, *Geoelectrical evidence of bicontinuum transport in groundwater.* Geophysical Research Letters, 2007. **34**(12).

Table 1 Overview of fluids

Brine	B10	10 g/L NaCl
	B35	35 g/L NaCl
Polymer solution	P10	1000 ppm, 10 g/L NaCl
	P35	1000 ppm, 35 g/L NaCl

Table 2 Conductivity of NaCl brines at 22.5˚C

Concentration [g/L]	Conductivity [mS/cm]
10	16.84
15	22.79
20	31.90
25	39.50
30	45.60
35	53.60

Table 3 Average properties of the sandpack. The values are estimated from 12 sandpacks.

Properties of sandpack column		
Length	L	80 cm
Diameter	D	1.5 cm
Grain size	d_{macro}	63-200 µm
Micro grain size	d_{micro}	80 nm
Pore size		6 nm
Surface area		500 m^2/g
Total porosity	ϕ_{total}	82 %
Macro porosity	ϕ_{macro}	44 %
Micro porosity	ϕ_{micro}	38 %
Permeability	k	6.835 D
Formation resistivity factor	F	1.8626
Tortuosity	τ	1.529
Cementation factor	m	1.0

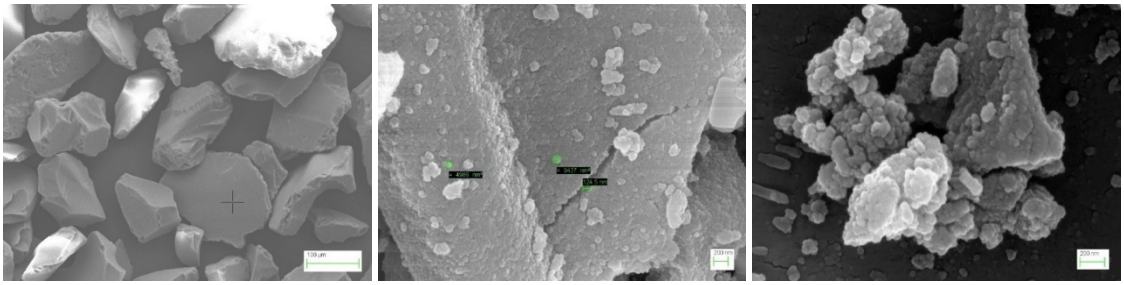

Figure 1 The Silica Gel grains. a) Overview of the sand grains, b) the surface of one grain, the size of the micro grains is 80 nm and the fracture measures 126 – 200 nm, c) the micro structure close-up, every grain is a rigid network of silica grains consolidated together. The pictures are taken with SEM at UiS.

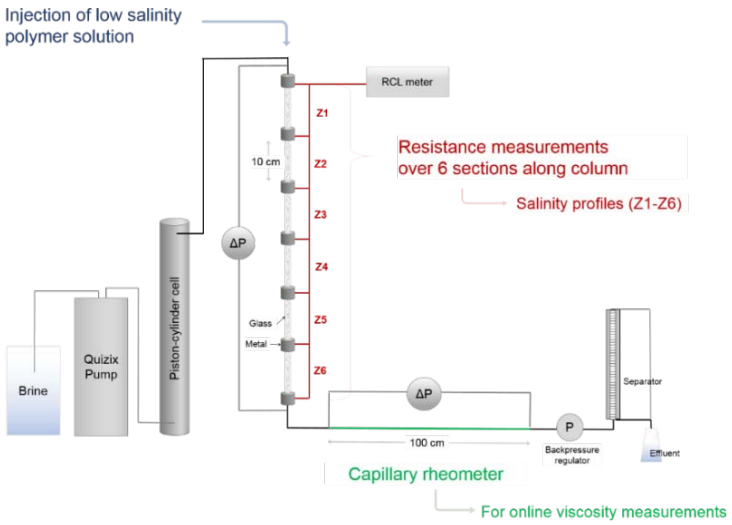

Figure 2 The experimental set-up, the sandpack was flooded from the top. The electric resistance was measured over 6 glass sections, and a capillary tube rheometer connected at the outlet of the column was used to measure the viscosity of effluent fluid.

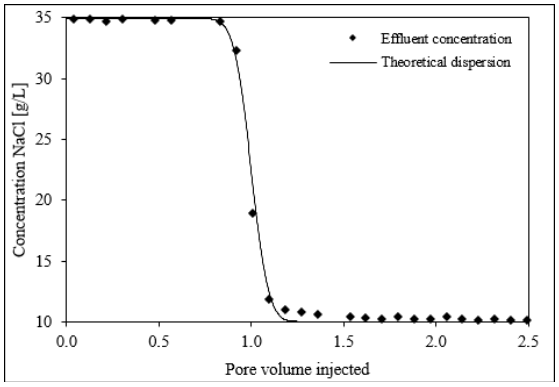

Figure 3 Displacing B35 by B10. Effluent salinity concentration profile.

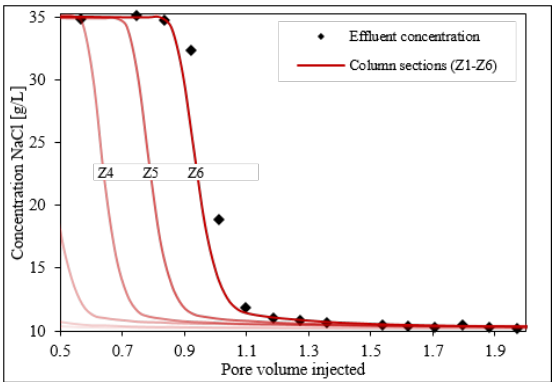

Figure 4 Effluent and calculated concentrations from resistance measurements

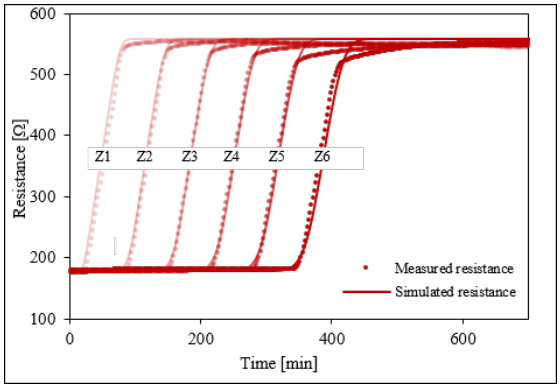

Figure 5 The electric resistance in the 6 sections along the sandpack during P10 injection at 0.3 ml/min. The circles are experimental data and the solid lines represents simulated data.

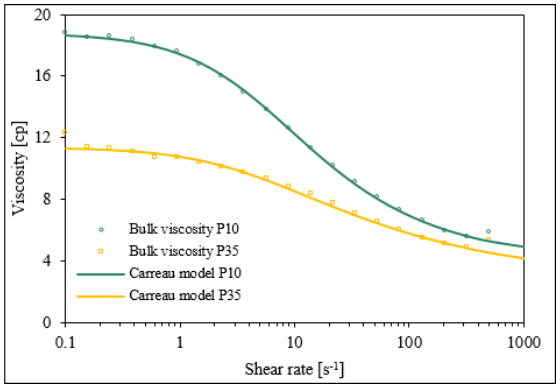

Figure 6 Bulk rheology of polymer solution P10 and P35 in rheometer (plate and cone).

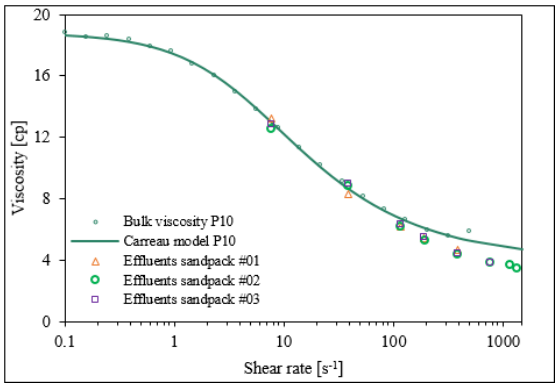

Figure 7 Bulk measurements and effluent viscosity from capillary tube rheometer of P10 at various injection rates in 3 different experiments.

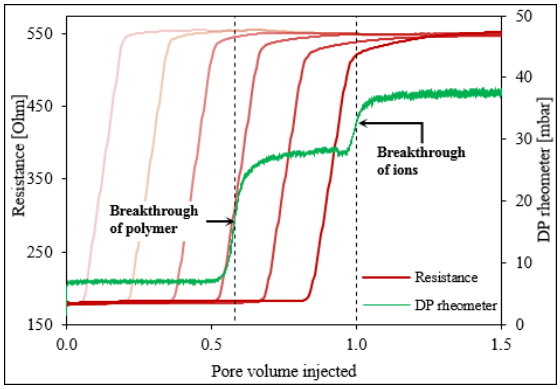

Figure 8 The pressure difference over the capillary tube rheometer and the corresponding resistance measurements along the sandpack column during P10 injection at 0.3 ml/min.

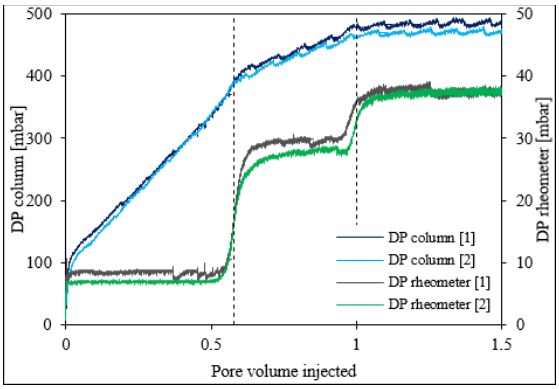

Figure 9 The pressure difference across the sandpack and across the capillary tube rheometer during P10 injection at 0.3 ml/min. [1] and [2] represent the first and the second injection.

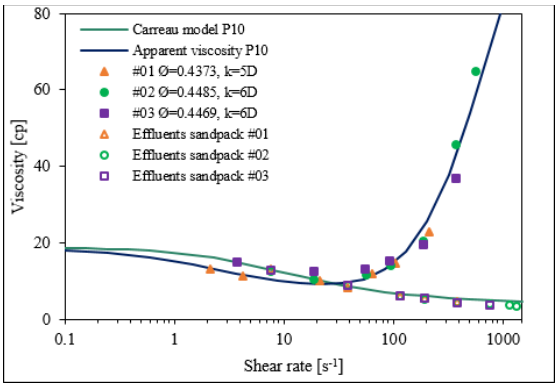

Figure 10 The apparent viscosity of P10 in-situ and in the capillary tube rheometer versus shear rates. The apparent viscosity in-situ is shear thickening, while the effluent is shear thinning.

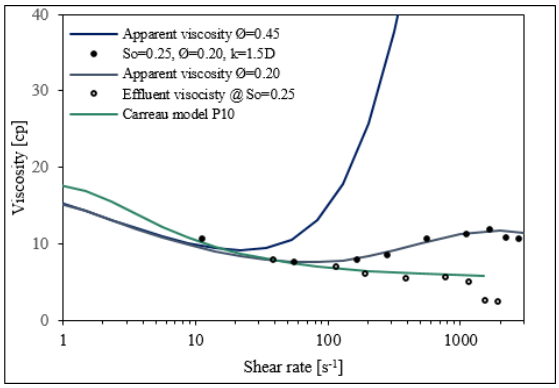

Figure 11 The apparent viscosity of P10 in-situ and in the capillary tube rheometer versus shear rates when oil was present in pores ($S_w \approx 75$ %).